



Published in final edited form as:

*Radiother Oncol.* 2014 June ; 111(3): 360–365. doi:10.1016/j.radonc.2014.06.001.

## Recurrences after intensity modulated radiotherapy for head and neck squamous cell carcinoma more likely to originate from regions with high baseline [18F]-FDG uptake

Anne K Due<sup>1</sup>, Ivan R Vogelius<sup>1</sup>, Marianne C Aznar<sup>1,2</sup>, Søren M Bentzen<sup>1,3</sup>, Anne K Berthelsen<sup>1,5</sup>, Stine S Korreman<sup>2,4</sup>, Annika Loft<sup>5</sup>, Claus A Kristensen<sup>1</sup>, and Lena Specht<sup>1</sup>

<sup>1</sup>Department of Radiation Oncology, Rigshospitalet, University of Copenhagen, Copenhagen, Denmark

<sup>2</sup>Niels Bohr Institute, University of Copenhagen, Copenhagen, Denmark

<sup>3</sup>Department of Human Oncology and Medical Physics, University of Wisconsin, Madison, WI

<sup>4</sup>Department of Science, Systems and Models, Roskilde University, Roskilde, Denmark

<sup>5</sup>Department of Clinical Physiology, Nuclear Medicine & PET, Rigshospitalet, University of Copenhagen, Copenhagen, Denmark

### Abstract

**Background and Purpose**—To analyze the recurrence pattern in relation to target volumes and <sup>18</sup>F-fluorodeoxyglucose (FDG) uptake on positron emission tomography in head and neck squamous cell carcinoma (HNSCC) patients treated with definitive chemoradiation.

**Material and Methods**—520 patients received radiotherapy for HNSCC from 2005–2009. Among 100 patients achieving complete clinical response and a later recurrence, 39 patients with 48 loco-regional failures had a recurrence CT scan before any salvage therapy. The estimated point of origin of each recurrence was transferred to the planning CT by deformable image co-registration. The recurrence position was then related to the delineated target volumes and iso-SUV-contours relative to the maximum standard uptake value (SUV). We defined the recurrence density as the total number of recurrences in a sub-volume divided by the sum of that volume for all patients.

**Results**—54% (95% CI 37–69%) of recurrences originated inside the FDG-positive volume and 96% (95% CI 86–99%) in the high dose region. Recurrence density was significantly higher in the central target volumes ( $P < 0.0001$ ) and increased with increasing FDG avidity ( $P = 0.036$ ).

© 2014 Elsevier Ireland Ltd. All rights reserved.

Corresponding author: Ivan Richter Vogelius, Department of Radiation Oncology, Section 3994, Rigshospitalet, Blegdamsvej 9, Denmark – 2100 Copenhagen, ivan.storgaard.vogelius@rh.regionh.dk, Phone: +45 3545 9885, Fax: +45 3545 3990.

**Publisher's Disclaimer:** This is a PDF file of an unedited manuscript that has been accepted for publication. As a service to our customers we are providing this early version of the manuscript. The manuscript will undergo copyediting, typesetting, and review of the resulting proof before it is published in its final citable form. Please note that during the production process errors may be discovered which could affect the content, and all legal disclaimers that apply to the journal pertain.

### Conflicts of interest statement

The authors have no conflicts of interest to disclose.

**Conclusions**—The detailed pattern-of-failure data analysis suggest that most recurrences occur in the FDG PET positive areas or the solid tumor.

### Keywords

Head and neck cancer; recurrence; pattern of failure; FDG-PET; radiotherapy

---

## Introduction

Recent years have seen a number of promising developments in medical imaging with the aim of identifying spatial variation in resistance to therapy. This is of particular interest in radiation oncology where the anti-cancer agent, ionizing radiation, can be modulated in space and time. The rationale is to increase the prescribed dose selectively in those regions of the tumor that have a high likelihood of failing after standard dose of (chemo-)radiation therapy. Planning and delivery of such non-uniform dose prescriptions is referred to as radiation dose painting (1–3). Modeling studies suggest that dose painting could substantially improve locoregional outcome without the increase in toxicity associated with uniform dose escalation (4–6).

Most attempts at identifying and validating a candidate imaging biomarker of radioresistance, for example radiolabeled tracers for positron emission tomography (PET) (7), have taken a “bottom-up” approach, focusing on putative mechanistic links between the imaging biomarker and radioresponsiveness. Here, we propose a “top-down” approach based on analysis of the spatial variability in the observed risk of loco-regional tumor recurrence after radiotherapy. The advantage of the latter approach is that it does not rely on any assumptions on the mechanism behind image intensity variations. The disadvantage is that the clinical-outcome driven method requires a relatively large cohort of patients with long follow-up. This paper tests the potential of FDG uptake before treatment as a potential biomarker of loco-regional recurrence risk. FDG uptake is a complex function of many factors (8), but if an empirical correlation between FDG uptake and local recurrence risk could be demonstrated in a large clinical series, this would identify FDG uptake as a promising dose painting target.

We recently hypothesized that loco-regional recurrences in patients who achieved a complete remission after primary therapy are likely to originate from a focal point or at least a limited volume (9). This focal pattern of local-regional failure serve as the empirical base for testing for correlations between target volumes or FDG avidity and the density of failures in the current study.

## Material and methods

### Patients

Patients receiving IMRT for head and neck cancer at Rigshospitalet, University of Copenhagen, Denmark, between January 2005 and December 2009 were considered for this study. Inclusion criteria were: 1) HNSCC of the oral cavity, pharynx or larynx; 2) treated with curatively intended IMRT; 3) complete clinical response after initial treatment; 4)

biopsy verified loco-regional recurrence; and 5) CT scan of recurrence before any salvage therapy attempt. Exclusion criteria were: previous treatment for cancer in the area, surgery prior to radiotherapy, a synchronous cancer, or confirmed distant metastases at time of treatment. Ethics approval is not required by Danish law as the research is based on retrospective review of non-biological data of routinely treated patients.

All patients with oral cavity cancer were carefully assessed for primary surgery by a surgeon and only medically inoperable patients or patients refusing surgery were offered primary (chemo-)radiotherapy and allowed inclusion.

### **Primary tumor: Treatment planning and delivery**

For all patients, except one, the treatment planning scans were performed on a hybrid PET/CT scanner. All patients were immobilized in supine position on a flat scanner couch using an individually moulded mask covering head and shoulders. After six hours of fasting, 400 MBq FDG was injected intravenously. The patients were scanned one hour after FDG injection according to the department protocol. Intravenous contrast agent was used for the CT scan unless contraindicated.

Several target volumes were delineated in each patient with every volume encompassing the volume previously delineated (i.e. nested volumes) following local guidelines (cf. Table 1) adapted from the recommendations by the Danish Head and Neck Cancer Group (DAHANCA). PET positive volumes were delineated in collaboration with a nuclear medicine physician based on visual assessment (ie. not using auto-contouring thresholds except for a first estimation). PET positive lymph node volumes were included in the corresponding target volume, GTV(FDG, clinical). GTV(all image, clinical) was delineated in collaboration with a radiologist based on all available imaging data and clinical examination. GTV(all image, clinical) includes involved lymph nodes without FDG uptake. The total prescribed radiation dose to the CTV-t was 66/68 Gy in 33/34 fractions, 6 fractions per week (cf. Table 1). Tumors with a diameter > 4 cm and primary nasopharyngeal tumors were prescribed 68 Gy. A minimum of 60 Gy was prescribed to CTVE-h, and 50 Gy to the CTVE-l. Radiation was delivered as a simultaneous integrated boost with 2 Gy per fraction to the CTV-t. IMRT was planned on the Varian Eclipse dose planning system with a sliding window technique and, in general, 6MV photon beams. Dose was delivered on Varian Linear accelerators with position verified by weekly portal imaging. Total dose was in general prescribed as mean dose to the planning target volume with the highest dose, albeit small adjustments was allowed to ensure the required coverage of the planning target volume with the 95% isodose line. The two lower dose levels were generally approved by ensuring coverage of the 95% isodose line - see (6) for details. Administration of daily Nimorazol (1200mg/m<sup>2</sup>) and weekly Cisplatin (40 mg/m<sup>2</sup>) also followed the DAHANCA guidelines.

### **Recurrence: recurrence scan and delineation of recurrence volume**

Clinical treatment response was evaluated two months after completed radiotherapy. Hereafter, follow-up visits were scheduled every four months for two years and then every six months for the following three years. In the event of a suspected recurrence, a CT was

performed at the patient's local hospital using a standard scanner couch. Recurrence volumes were delineated by a radiologist and an oncologist with access to all previous imaging and clinical examinations available at the time of recurrence.

### Co-registration, recurrence origin, and density

An estimated point of origin (Nidus) was defined as the point within the recurrence volume for which the *maximum* distance to the boundary of the recurrence volume was smaller than for any other point in the recurrence volume (9).

Intensity-based deformable co-registrations of the recurrence CT and the planning CT were performed by a radiologist, using Velocity version 2.6.1 (Velocity Medical Solutions, Atlanta, GA). This enabled the Nidus on the recurrence CT to be related to the target volumes on the planning PET/CT, cf. Figure 1. The reproducibility of the entire process, including delineation of the recurrence, deformable image registration and assignment of the focal origin was studied in a previous publication (9) with estimated differences of independent double determinations of 0.7 cm on average. The number of recurrence origins in a target volume can be described as (i) the number of recurrence origins *specific* to a target volume or region of interest (ROI) or (ii) the number of recurrence origins *inside* a ROI. The number of recurrences for which the estimated point of origin is *specific* to a ROI will be the number of recurrences within the ROI excluding the recurrences located in other target volumes encompassed by the ROI in question. The number of recurrences *inside* a ROI will include also the recurrences located in other target volumes encompassed by the ROI in question.

The maximum standardized uptake value (SUV) within the GTV(FDG, clinical) was recorded and used for construction of sub-volumes within GTV(FDG, clinical) as iso-SUV-contours relative to the maximum SUV. The recurrence density was calculated as the total number of recurrences in a volume divided by the summed volume of the all the corresponding target volumes for all 39 patients:

$$\text{Recurrence density} = \frac{\text{total number of recurrences inside a ROI}}{\text{pooled volume of the ROI}(\text{cm}^3)}$$

### Statistics

Bootstrap resampling technique drawing 100,000 samples with replacement from the list of patients was used to estimate the 95% confidence interval (CI) for the recurrence density in each target volume as the range from the 2.5–97.5 percentile of the histogram of recurrence densities.

A correlation between the FDG uptake and recurrence density was tested by assigning a rank order to each of the iso-SUV-contours relative to the maximum SUV: the 50%-SUV max region is assigned the number 1; the 60%-SUV max region is assigned the number 2 etc. Again, 100000 bootstrap samples were drawn with replacement from the list of patients and the Spearman rank correlation coefficient,  $R_S$ , between recurrence density and the assigned number of the SUV regions was calculated for each bootstrap sample. A test for

$R_S = 0$  was obtained from the proportion of bootstrap samples with negative or zero correlation coefficient. A probability of 5 % or less was considered significant for rejecting the hypothesis of negative or no correlation. A similar approach was used to test for a correlation between the ordered list of target volumes (cf. table 1) and recurrence density.

## Results

Patient charts were retrieved throughout 2010. From 2005 to 2009, 520 patients received IMRT for head and neck cancer in the pharynx, larynx or oral cavity. 304 patients completed IMRT with curative intent and achieved a complete response, cf. Figure 2. The median follow-up of these 304 patients was 17 months from end of treatment to last follow-up or recurrence. The median time to censoring in patients without a prior recurrence was 1.7 years (range 20 days to 5.1 year). The 5-year Kaplan-Meier estimate of risk of locoregional recurrence after complete response was 29.6%. 39 patients with 48 recurrence volumes met the inclusion additional inclusion criteria, cf. Figure 2 and Table 2 (supplement). In one patient, two recurrence volumes had merged and the Nidus method could not be applied. Instead, the oncologist determined the most likely points of origin of the two recurrences within the recurrence volumes. Four patients had no GTV(FDG, clinical) delineated for their radiotherapy planning and four patients had no GTV(All image, clinical) delineated. For these recurrences, the relation to GTV(FDG, clinical) and GTV(All image, clinical) could not be analyzed, but the patients were retained in the rest of the analysis.

96% of recurrences (95% CI 86–99%) occurred inside the region with the highest prescribed dose, but the region with the highest prescribed dose on average encompassed only 29% of the total target (i.e. CTVE-1). 22 of 41 recurrences in patients with a delineated GTV(FDG, clinical) (54%, 95% CI 37–69%) occurred inside the GTV(FDG, clinical). The GTV(FDG, clinical) encompassed 12% of the high dose volume and only 4% of the total target volume on average. One recurrence was located out-of-field (2%, 95% CI: 0–11%).

Consequently, a higher recurrence density was observed in the high-dose target volumes, where GTV(FDG, clinical) accounted for the highest density ( $0.02 \text{ cm}^{-3}$ , 95% CI 0.014–0.028), cf. Figure 3 and 4. 47 recurrences were encompassed in the CTVE-1, but its large volume leads to a modest recurrence density ( $0.0015 \text{ cm}^{-3}$ , 95% CI 0.0013–0.0018). The correlation between recurrence density and target volume was strong, with more than 95% of the bootstrap samples resulting in a correlation coefficient of 1. For the sub volumes within GTV(FDG, clinical), the recurrence density was higher the closer the iso-SUV-curves were to the maximum SUV, cf. Figure 4. Recurrence density correlated significantly with percentage of SUV max ( $p=0.036$ ).

## Discussion

Overall treatment intensity of HNSCC is close to patient tolerance (10, 11) and new strategies are warranted in an attempt to optimize benefit/risk ratios at the individual patient level. Detailed patterns of failure studies can help determine where the radiation dose will help most in terms of prolonging the time to loco-regional progression. The method chosen for conducting pattern of failure studies in patients achieving complete response impacts the

conclusion (9, 12). We believe a focal method, as applied here, is preferable to volume overlap methods as volume overlap methods will push the recurrence assignments towards more peripheral target sub-volumes as the recurrence grows. However, there is still considerable uncertainty and reproducibility and accuracy is limited (9). The significant correlation between target volume and recurrence density shows that, despite shortcomings, the method is capable of detecting the structure of the recurrence pattern when a sufficient number of patients is included in the analysis. Modeling studies suggest that the optimal distribution of a certain integral dose is one which provides the same risk of failure for all sub-volumes of the tumor (4). Hence, the current data indicate that there is a potential for dose redistribution(6).

The introduction of highly conformal radiation therapy techniques caused concerns that marginal misses could become an issue (13, 14). These concerns are not supported by the current data as 96% (95% CI 86–99%) of the observed recurrences originate in the region prescribed to 66–68 Gy. This is in accordance with other investigations (14, 15). The vast majority of recurrences seem to be the result of insufficient dose delivered to parts of the selected target volumes. Therefore, dose painting becomes a compelling strategy if a spatial variation in local tumor control can be established (1). On a cautionary note, our department practice of adding 1 cm margin to the GTV(All image, clinical) should be kept in mind, and the proportion of recurrences in CTV-t may be higher with a smaller margin. An analysis of the spatial distribution of the recurrences *within* the CTV-t region would be interesting, but unfortunately we currently do not have the statistical power with only 10 recurrences in this region.

The recurrence density is a simple metric for comparing risk/benefit ratios for potential dose-painting targets. Here, the average volume of GTV(FDG, clinical) was 33 cm<sup>3</sup> and the mean volume of CTVE-1 is 822 cm<sup>3</sup>. Escalating the dose to CTVE-1 by just 2 Gy would require delivery of the same integral dose as escalating the dose to GTV(FDG, clinical) by 50 Gy! Modeling studies suggest that the optimal distribution of the same integral dose would be done by increasing the dose most to GTV(FDG, clinical), less to GTV(All image, clinical) and a little to CTV, while decreasing the dose to the elective volumes that are very large, but harbors few recurrences(6). Hence, this study provides strong support for current experimental strategies increasing the dose to FDG avid regions (16, 17).

One limitation to the current study is the heterogeneity of the patient cohort. P16 status of the tumor was, unfortunately, not available. However, it is important to notice that the implicit assumption behind this study is that the recurrence *pattern* across the HNSCC population is similar even in the presence of significant variation in absolute risk of local recurrence. At present relatively little is known about the pattern of relapse in HPV-related vs. non-HPV related HNSCC. Similarly, tumor subsite could influence the pattern of failure. Table 3 (supplement) shows no clear variability in failure pattern among tumor subsites, although the current study has very limited power to resolve a potential variation. Finally, the use of concomitant cisplatin based therapy could be speculated to affect the pattern of failure. However, with no evidence of a variation, we follow the principle of parsimony and analyze the data together.

Another important limitation of the current study is that the CT scans of the recurrences were prescribed on routine clinical indication rather than as a part of a systematic trial. 30 patients did not have an evaluable scan or a biopsy verified recurrence and these patients may be suspected to have bulky or multifocal disease. In other words, they could potentially have a different failure site distribution than the analyzable patients.

The present study analyzed data from patients who achieved a complete response on clinical examination after definitive (chemo)-RT. These patients are most likely to benefit from modest dose escalation as they are responding well to current therapy. In contrast, patients with persistent disease after initial radiotherapy are most likely harder to cure with a modest dose escalation or redistribution. However, as patients with persistent disease fail in the gross tumor volume, boosting the central part of the high dose target is also likely to increase the dose to the parts of the tumor that are not controlled in patients with persistent disease.

The ideal map of therapeutic efficacy from a pattern of failure study would be a map of the probability density of failing in specific sub-regions of the target, which can be derived prior to radiotherapy. Extension of the current estimates to account for time-to-event and competing risks is currently in progress but requires analysis of the large group of patients who have not failed at the last follow up.

Another limitation of the retrospective study design used here is the lack of fully standardized scanning protocols. Volumes considered in the present study are defined as contours relative to SUVmax, which probably diminishes this problem. Also, treatment protocols and follow-up policies were standardized during the period covered here. The advantage of the present study design is clearly the availability of mature failure data. In addition the quantification of the failure density is attractive for deriving prospective trial strategies as demonstrated by the modelling paper (6).

We make no effort to correlate the FDG uptake with underlying heterogeneities in tumor biology in the current paper, but this would certainly be an interesting research avenue to gain a deeper understanding of the mechanisms behind the pattern of recurrence.

## Conclusions

All but one of the recurrences occurred in-field, indicating that the current IMRT technique does not result in a high risk of geographical misses. A substantial variation in the density of recurrences between target volumes defined from pretreatment imaging was observed and this provides further stimulus for exploring FDG PET based dose painting strategies in HNSCC.

## Supplementary Material

Refer to Web version on PubMed Central for supplementary material.

## Acknowledgements

Supported by CIRRO - The Lundbeck Foundation Centre for Interventional Research in Radiation Oncology; University of Copenhagen; the Danish Graduate School for Clinical Oncology; and the Global Excellence in Health program of the Capital Region of Denmark. SMB acknowledges support from the National Cancer Institute grant no. 2P30 CA 014520-34.

## References

1. Bentzen SM. Theragnostic imaging for radiation oncology: dose-painting by numbers. *Lancet Oncol.* 2005; 6:112–117. [PubMed: 15683820]
2. Brahme A. Biologically optimized 3-dimensional in vivo predictive assay-based radiation therapy using positron emission tomography-computerized tomography imaging. *Acta Oncol.* 2003; 42:123–136. [PubMed: 12801131]
3. Ling CC, Humm J, Larson S, et al. Towards multidimensional radiotherapy (MD-CRT): biological imaging and biological conformality. *Int. J. Radiat. Oncol. Biol. Phys.* 2000; 47:551–560. [PubMed: 10837935]
4. Brahme A, Agren AK. Optimal dose distribution for eradication of heterogeneous tumours. *Acta Oncol.* 1987; 26:377–385. [PubMed: 3426851]
5. Sovik A, Malinen E, Bruland OS, et al. Optimization of tumour control probability in hypoxic tumours by radiation dose redistribution: a modelling study. *Phys. Med. Biol.* 2007; 52:499–513. [PubMed: 17202629]
6. Vogelius IR, Håkansson K, Due AK, et al. Failure-probability driven dose painting. *Med. Phys.* 2013; 40:081717. [PubMed: 23927314]
7. Bentzen SM, Gregoire V. Molecular imaging-based dose painting: a novel paradigm for radiation therapy prescription. *Semin. Radiat. Oncol.* 2011; 21:101–110. [PubMed: 21356478]
8. Jadvar H, Alavi A, Gambhir SS. 18F-FDG uptake in lung, breast, and colon cancers: molecular biology correlates and disease characterization. *J Nucl. Med.* 2009; 50:1820–1827. [PubMed: 19837767]
9. Due AK, Vogelius IR, Aznar MC, et al. Methods for estimating the site of origin of locoregional recurrence in head and neck squamous cell carcinoma. *Strahlenther. Onkol.* 2012; 188:671–676. [PubMed: 22580623]
10. Bentzen SM, Rosenthal DI, Weymuller EA, et al. Increasing toxicity in nonoperative head and neck cancer treatment: investigations and interventions. *Int. J. Rad. Oncol. Biol. Phys.* 2007; 69:S79–S82.
11. Trotti A. Toxicity in head and neck cancer: a review of trends and issues. *Int. J. Radiat. Oncol. Biol. Phys.* 2000; 47:1–12. [PubMed: 10758302]
12. Raktveit SA, Dehdashti H, Raaijmakers CP, et al. Origin of Tumor Recurrence After Intensity Modulated Radiation Therapy for Oropharyngeal Squamous Cell Carcinoma. *Int. J. Radiat. Oncol. Biol. Phys.* 2012
13. Mendenhall WM, Amdur RJ, Palta JR. Intensity-modulated radiotherapy in the standard management of head and neck cancer: promises and pitfalls. *J Clin. Oncol.* 2006; 24:2618–2623. [PubMed: 16763274]
14. Soto DE, Kessler ML, Pierris M, et al. Correlation between pretreatment FDG-PET biological target volume and anatomical location of failure after radiation therapy for head and neck cancers. *Radiother. Oncol.* 2008; 89:13–18. [PubMed: 18555547]
15. Dirix P, Vandecasteele V, De Keyser F, et al. Dose painting in radiotherapy for head and neck squamous cell carcinoma: value of repeated functional imaging with (18)F-FDG PET, (18)F-fluoromisonidazole PET, diffusion-weighted MRI, dynamic contrast-enhanced MRI. *J. Nucl. Med.* 2009; 50:1020–1027. [PubMed: 19525447]
16. Madani I, Duthoy W, Derie C, et al. Positron emission tomography-guided, focal-dose escalation using intensity-modulated radiotherapy for head and neck cancer. *Int. J. Radiat. Oncol. Biol. Phys.* 2007; 68:126–135. [PubMed: 17448871]



17. Madani I, Duprez F, Boterberg T, et al. Maximum tolerated dose in a phase I trial on adaptive dose painting by numbers for head and neck cancer. *Radiother.Oncol.* 2011; 101:351–355. [PubMed: 21742392]

Author Manuscript

Author Manuscript

Author Manuscript

Author Manuscript

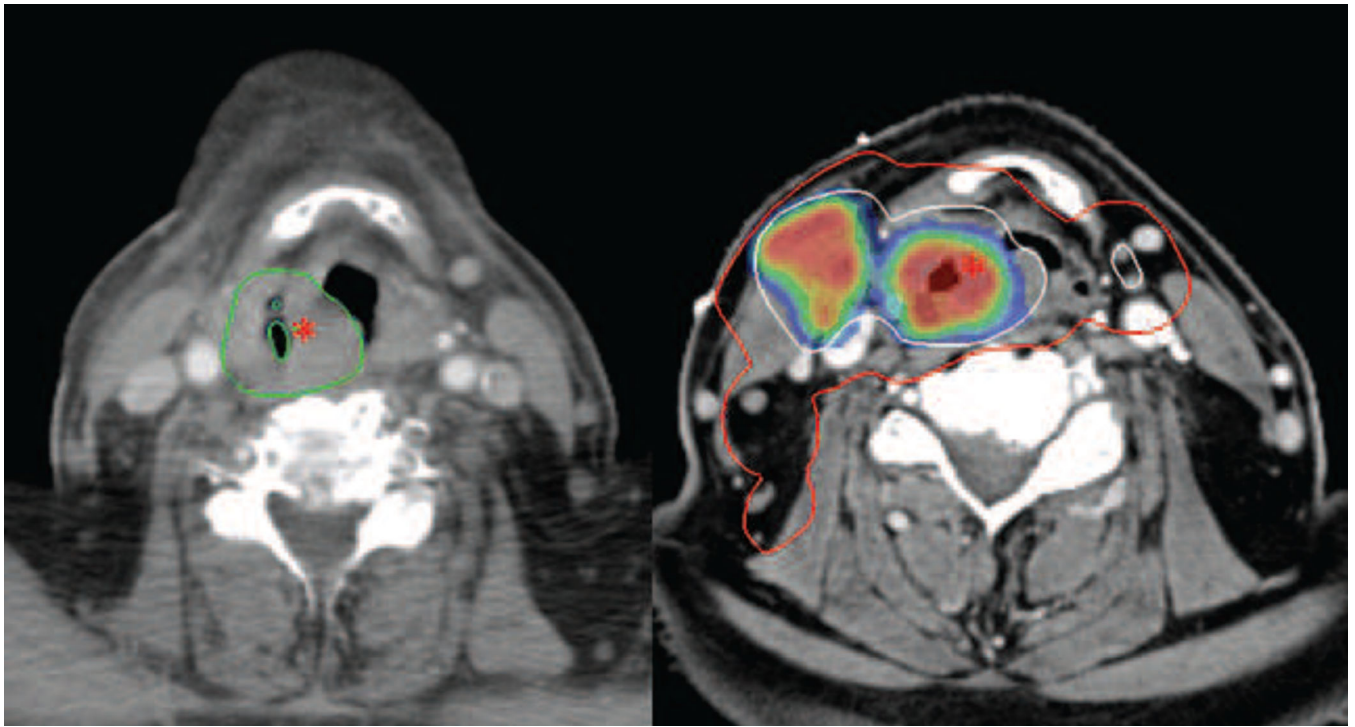


**Figure 1.**

Patient with a hypopharyngeal cancer (T3 N2c M0) treated with intensity modulated radiation therapy with concomitant Cisplatin and Nimorazol. Left: CT scan at time of recurrence, 7 months after completion of radiation therapy. The recurrence volume is delineated in green and the asterisk marks the location of the estimated recurrence origin (Nidus). Right: The PET/CT treatment planning scan. The GTV(All image, clinical) is delineated in white and encompassed by the CTV-t delineated in red. The asterisk marks the location of the Nidus, transferred from the recurrence scan by deformable co-registration. The color wash illustrates FDG-PET avidity. GTV(All image, clinical): Gross tumor volume. CTV-t: Clinical target volume of primary tumor.

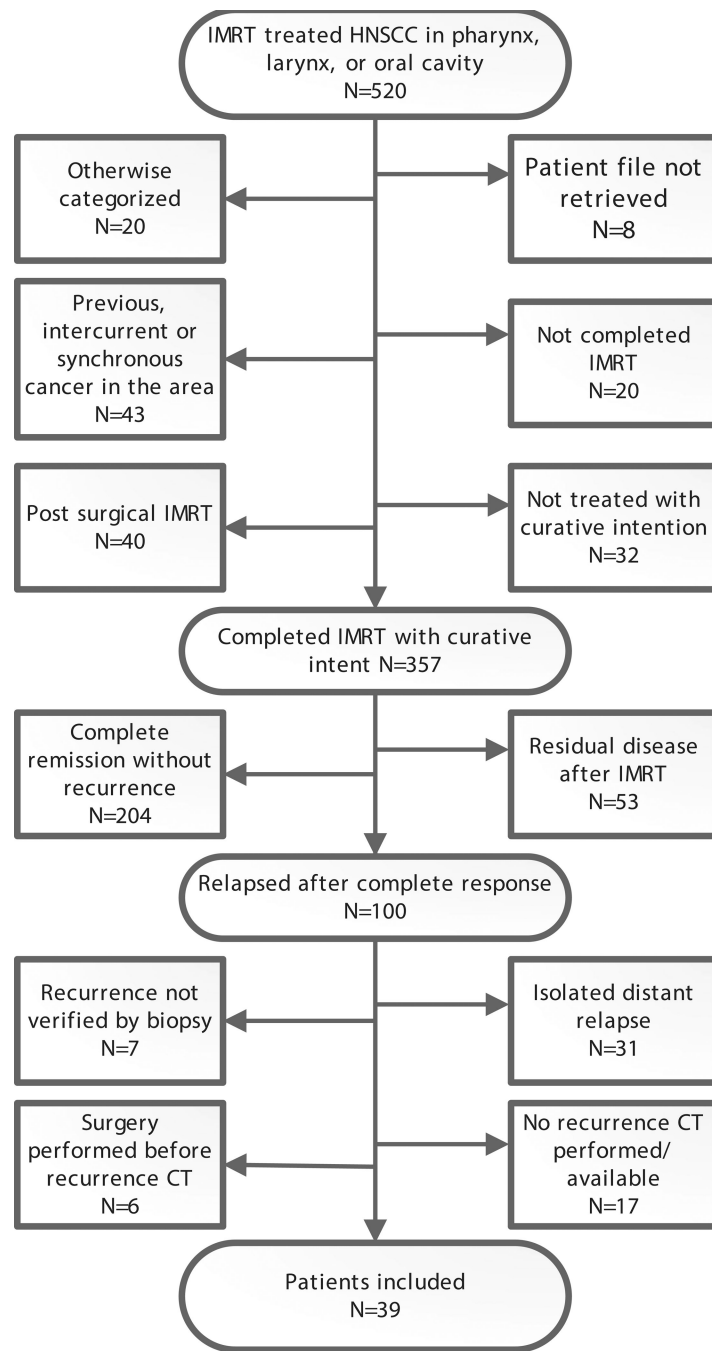


**Figure 2.** Flowchart for all patients receiving intensity modulated radiotherapy (IMRT) for head and neck squamous cell carcinoma during the period 2005–2009.

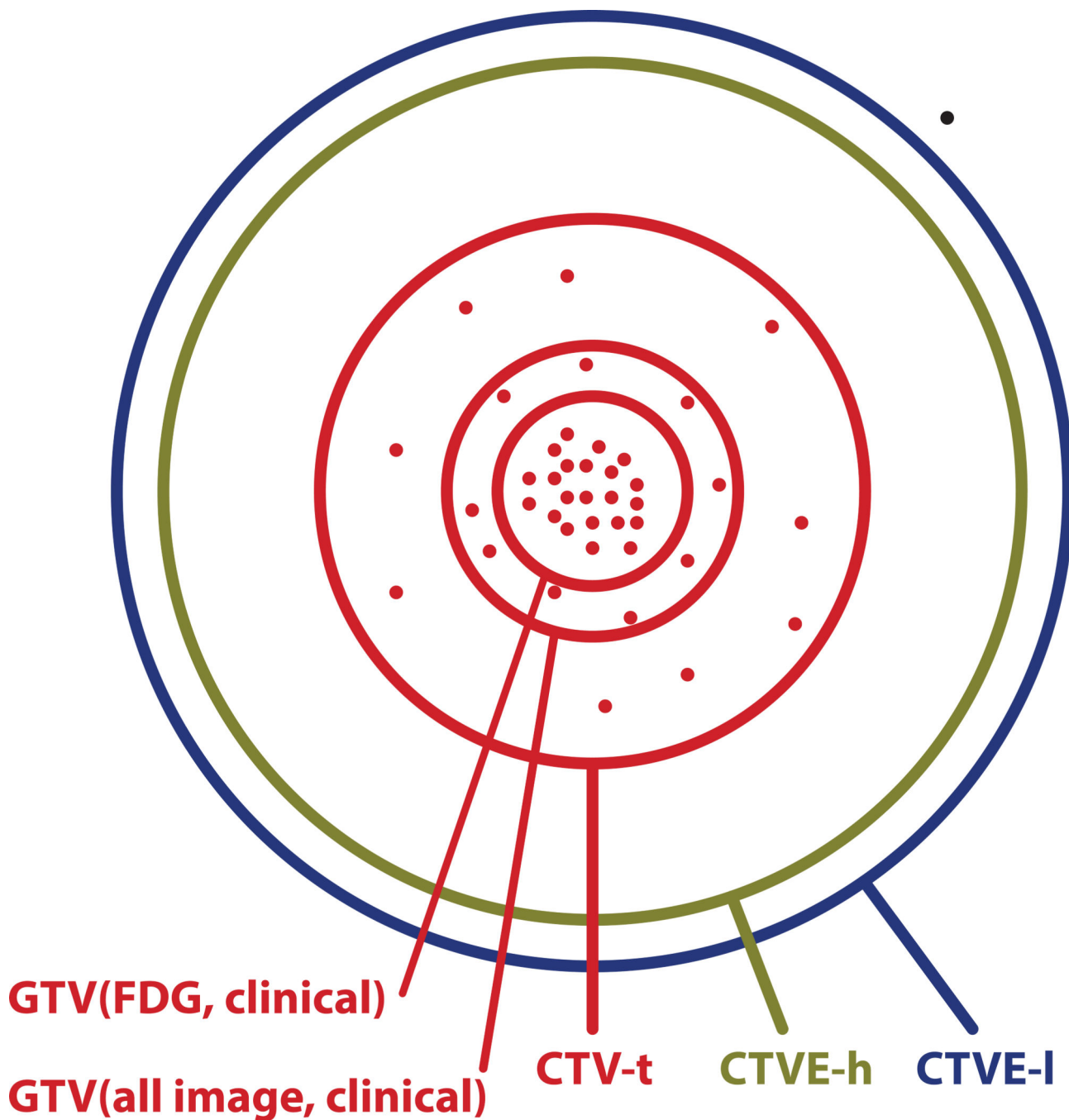


**Figure 3.** Schematic representation of the location of 41 recurrences (dots) in the 35 patients with a GTV(FDG, clinical) in relation to the target volumes defined at the time of treatment planning. Areas of circles are proportional to the average physical volume of the corresponding treatment volume. Red lines indicate target volumes receiving 66/68 Gy; green line: 60 Gy; and blue line: 50 Gy.

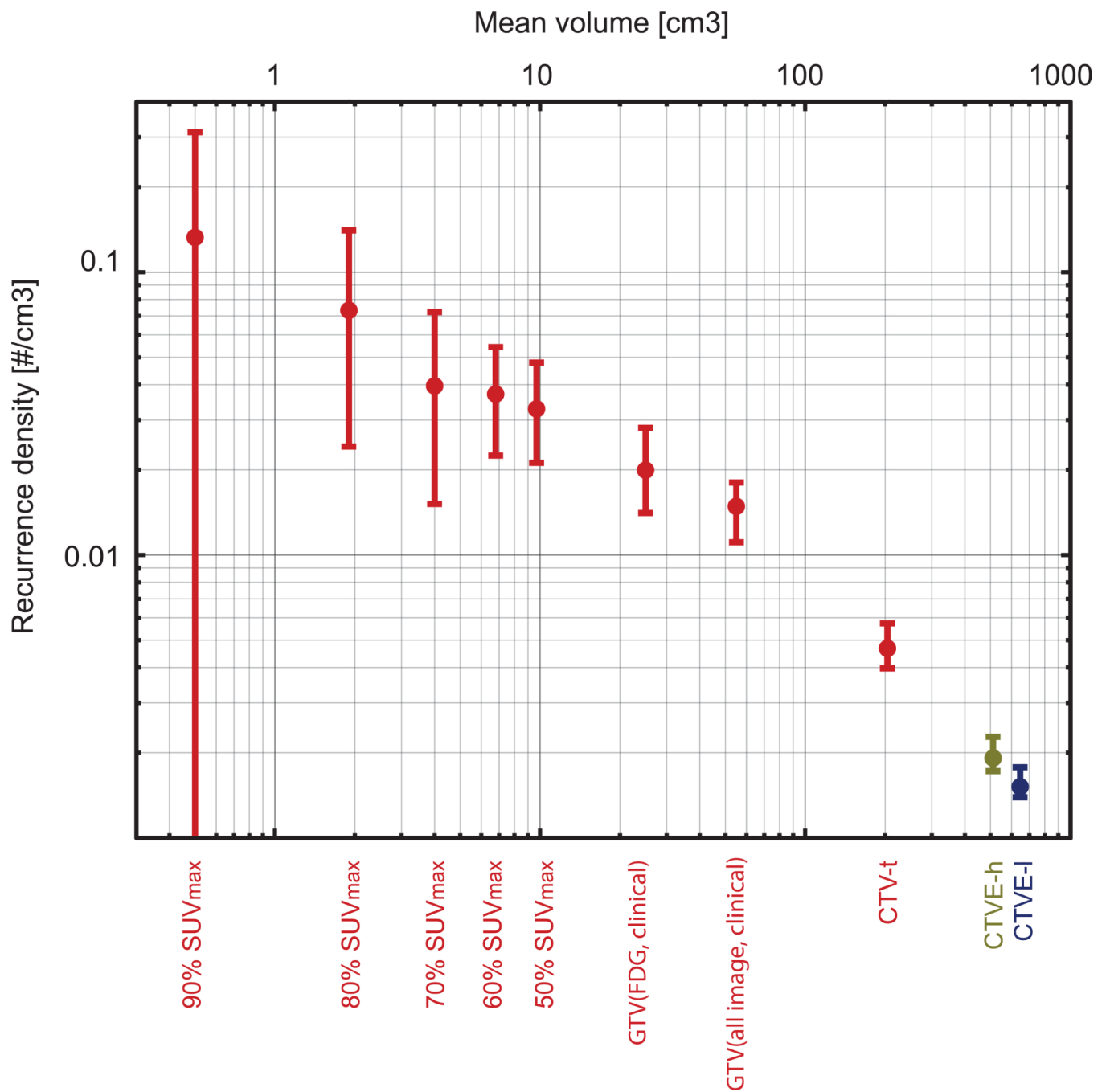


**Figure 4.** Recurrence density as no. of recurrences per cm<sup>3</sup> for target (sub)volumes with 95% CI. Colors indicate radiation dose levels, red: 66/68 Gy, green: 60 Gy, and blue: 50 Gy. If the risk of a local recurrence in a specific sub-region had been independent of the relative FDG SUV, the densities from 50% SUV<sub>max</sub> to 90% SUV<sub>max</sub> should have been constant.

**Table 1**

Definitions, regions of interest and location of recurrences.

Region of interest (ROI)	Definition	Dose*	No. of recurrences inside the ROI**	Recurrences specific to the ROI*** / recurrences available for analysis (%)	Median target volume cm <sup>3</sup> (range)
GTV-PET	The FDG-PET positive volume, delineated by a nuclear medicine physician.	66/68 Gy	22	22/41 (54)	22 (1–167)
GTV	The gross tumour volume, based on all available diagnostic imaging as well as the results of the clinical examination.		36	14/44 (32)	60 (7–245)
CTV-t	The clinical target volume includes the GTV with a 1 cm margin to account for delineation uncertainty, adjusted for unaffected bone and with a 3 mm margin to the skin.		46	10/48 (21)	244 (28–617)
CTVE-h	The high-risk elective clinical target volume includes areas at high risk of microscopic disease. It is constructed by adding a 2 mm margin to the CTV-t and including lymph node levels with a high risk of sub clinical disease.	60 Gy	47	1/48 (2)	598 (257–1444)
CTVE-l	The low-risk elective clinical target volume includes areas at low but still significant risk of microscopic disease. It is constructed by adding a 2 mm margin to CTVE-h and including lymph node levels with a low risk of sub clinical disease.	50 Gy	47	0/48 (0)	739 (413–1470)
Out-of-field	Anatomical regions outside of CTVE-l	-	48	1/48 (2)	-
GTV-PET 90%-SUVmax	GTV-PET sub-volumes defined by iso-SUV-curves constructed as percentages of the maximum SUV.		3	3/41 (7)	0.4 (0–2.6)
GTV-PET 80%-SUVmax		6	3/41 (7)	1.6 (0.1–11.7)	
GTV-PET 70%-SUVmax		7	1/41 (2)	3.4 (0.4–26.2)	
GTV-PET 60%-SUVmax		11	4/41 (10)	6.1 (0.7–43.1)	
GTV-PET 50%-SUVmax		14	3/41 (7)	9.2 (0.8–63.5)	
Other					
Recurrence volume	Delineated by the radiologist and radiation oncologist with access to all previous imaging and clinical examinations available at the time of recurrence volume.				
Nidus	Estimated point of origin within the recurrence volume minimizing the maximum distance to the recurrence boundary.				

\* According to the DAHANCA guidelines the prescribed total radiation dose to the CTV-t was 66 Gy, whereas tumors with a diameter > 4 cm and nasopharyngeal tumors were prescribed 68 Gy.

\*\* The number of recurrences *inside* a ROI also includes the recurrences located in the target volumes encompassed by the ROI in question.

\*\*\* The number of recurrences for which the estimated point of origin is *specific to* a ROI is the number of recurrences within that ROI but excluding recurrences located in target volumes contained inside the ROI in question.